PB-251 671

AN INVESTIGATION OF GAS PHASE OZONOLYSIS REACTIONS

California Polytechnic State University

Prepared for:

Environmental Sciences Research
Laboratory

March 1976

DISTRIBUTED BY:

NTIS

National Technical Information Service
U. S. DEPARTMENT OF COMMERCE

111034

EPA-600/3-76-024
March 1976

PB 251 671

Ecological Research Series

TECHNICAL REPORT DATA
(Please read Instructions on the reverse before completing)

1. REPORT NO. EPA-600/3-76-024	2.
3. RECIPIENT'S ACCESSION NO. PB-251 671	
4. TITLE AND SUBTITLE AN INVESTIGATION OF GAS PHASE OZONOLYSIS REACTIONS	5. REPORT DATE March 1976
	6. PERFORMING ORGANIZATION CODE
7. AUTHOR(S) David G. Williamson	8. PERFORMING ORGANIZATION REPORT NO.
9. PERFORMING ORGANIZATION NAME AND ADDRESS Chemistry Department, California Polytechnic State University, San Luis Obispo, California 93407	10. PROGRAM ELEMENT NO. 1AA008
	11. CONTRACT/GRANT NO. Grant No. R-800984
12. SPONSORING AGENCY NAME AND ADDRESS Environmental Sciences Research Laboratory, Office of Research and Development, U.S. Environmental Protection Agency, Research Triangle Park, NC 27711	13. TYPE OF REPORT AND PERIOD COVERED Final
	14. SPONSORING AGENCY CODE EPA-ORD
15. SUPPLEMENTARY NOTES	

16. ABSTRACT

A simple gas phase stopped-flow apparatus has been used to determine the rates and stoichiometry for the reactions of ozone with ethylene, propene, 1-butene, methylpropene, cis-2-butene, and trans-2-butene.

Measurements of the intensity of light scattered by aerosols generated by the reaction of ozone with trans-2-butene and with ethylene were made as a function of reaction time and initial reactant concentration.

PRICES SUBJECT TO CHANGE

17. KEY WORDS AND DOCUMENT ANALYSIS

a. DESCRIPTORS	b. IDENTIFIERS/OPEN ENDED TERMS	c. COSATI Field/Group
Air pollution Tests * Reaction kinetics * Stoichiometry * Ozonization * Alkene hydrocarbons		13B 14B 07D 07C

18. DISTRIBUTION STATEMENT RELEASE TO PUBLIC	19. SECURITY CLASS (This Report) UNCLASSIFIED	21. NO. OF PAGES 55
	20. SECURITY CLASS (This page) UNCLASSIFIED	22. PRICE $4.50-2.25

EPA Form 2220-1 (9-73)

EPA-600/3-76-024
March 1976

AN INVESTIGATION OF GAS PHASE OZONOLYSIS REACTIONS

by

David G. Williamson
Chemistry Department
California Polytechnic State University
San Luis Obispo, CA 93407

Grant No. R-900984

Project Officer

Joseph J. Bufalini
Atmospheric Chemistry and Physics Division
Environmental Sciences Research Laboratory
Research Triangle Park, North Carolina 27711

U.S. ENVIRONMENTAL PROTECTION AGENCY
OFFICE OF RESEARCH AND DEVELOPMENT
ENVIRONMENTAL SCIENCES RESEARCH LABORATORY
RESEARCH TRIANGLE PARK, NORTH CAROLINA 27711

ia

RESEARCH REPORTING SERIES

Research reports of the Office of Research and Development, U.S. Environmental Protection Agency, have been grouped into five series. These five broad categories were established to facilitate further development and application of environmental technology. Elimination of traditional grouping was consciously planned to foster technology transfer and a maximum interface in related fields. The five series are:

1. Environmental Health Effects Research
2. Environmental Protection Technology
3. Ecological Research
4. Environmental Monitoring
5. Socioeconomic Environmental Studies

This report has been assigned to the ECOLOGICAL RESEARCH series. This series describes research on the effects of pollution on humans, plant and animal species, and materials. Problems are assessed for their long- and short-term influences. Investigations include formation, transport, and pathway studies to determine the fate of pollutants and their effects. This work provides the technical basis for setting standards to minimize undesirable changes in living organisms in the aquatic, terrestrial, and atmospheric environments.

This document is available to the public through the National Technical Information Service, Springfield, Virginia 22161.

DISCLAIMER

This report has been reviewed by the Environmental Sciences Research Laboratory, U.S. Environmental Protection Agency, and approved for publication. Approval does not signify that the contents necessarily reflect the views and policies of the U.S. Environmental Protection Agency, nor does mention of trade names or commercial products constitute endorsement or recommendation for use.

CONTENTS

List of Figures iv

List of Tables v

I. Summary and Conclusions 1

II. Experimental Methods 5

III. Results and Discussion 11

1. Stoichiometry of some ozone-olefin reactions 11

2. Rates of ozone-olefin reactions 21

3. Measurements of light scattering by aerosols in the reaction of trans-2-butene with ozone 40

IV. References 46

LIST OF FIGURES

		Page
Figure 1.	Schematic of Apparatus	6
Figure 2.	Diagram of Reaction Cell	7
Figure 3.	n vs. $(Ethylene)_o/(O_3)_o$	16
Figure 4.	n vs. $(Propene)_o/(O_3)_o$	17
Figure 5.	n vs. $(1\text{-}Butene)_o/(O_3)_o$	18
Figure 6.	n vs. $(Cis\text{-}2\text{-}Butene)_o/(O_3)_o$	19
Figure 7.	n vs. $(Methylpropene)_o/(O_3)_o$	20
Figure 8.	Second Order Plot. Ethylene + Ozone	23
Figure 9.	Second Order Plot. Propene + Ozone	24
Figure 10.	Second Order Plot. 1-Butene + Ozone	25
Figure 11.	Second Order Plot. Methylpropene + Ozone	26
Figure 12.	Second Order Plot. Trans-2-Butene + Ozone	32
Figure 13.	Second Order Plot. Cis-2-Butene + Ozone	33
Figure 14.	Second Order Plot. Trans-2-Butene + Ozone. High Concentration	34
Figure 15.	Test for Inhibition of O_3 Decomposition	35
Figure 16a.	Infrared Spectrum of the Aerosol from the Trans-2-Butene + Ozone Reaction	38
Figure 16b.	Infrared Spectrum of the Aerosol from the Trans-2-Butene + Ozone Reaction	39
Figure 17.	Intensity of Scattered Light vs. Time in the Trans-2-Butene + Ozone Reaction	42
Figure 18.	Maximum Intensity of Scattered Light vs. Concentration of Trans-2-Butene	43

LIST OF TABLES

		Page
Table 1.	A Summary of Some Rate Constants for Ozone-Olefin Reactions	2
Table 2.	A Summary of the Rate Constants for Ozone-Olefin Reactions as Determined in this Study	3
Table 3.	The Stoichiometry of Some Ozone-Olefin Reactions	12
Table 4.	Apparent Second Order Rate Constants for Some Ozone-Olefin Reactions	27-28
Table 5.	Apparent Second Order Rate Constants for the Reaction of Trans-2-butene and Cis-2-butene with Ozone	31
Table 6.	Results of Light Scattering Experiments for the Ozone + Trans-2-butene Reaction	41
Table 7.	Light Scattering in the Ethylene + Ozone Reaction	44

SECTION I

SUMMARY AND CONCLUSIONS

This study was primarily designed to resolve the discrepancies which exist in the values of the second order rate constants for various ozone-olefin reactions. A brief summary of rate constants for some reported ozone olefin reactions, as adapted from references [2, 7], is shown in Table 1. The largest discrepancies in the second order rate constants shown in Table 1 are in the cases of cis and trans-2-butene.

A gas phase stopped-flow system was used to measure the rates and stoichiometry for the reactions of ozone with the above mentioned olefins. The stoichiometry for the reaction of ethylene, 1-butene, and methylpropene was found to depend on the ratio of initial concentrations $(\text{olefin})_o/(O_3)_o$. As this ratio increases the value of moles olefin used/moles ozone used, symbolized by n, increases. This suggests that the initial reactants are not only consumed by a bimolecular process between olefin and ozone, but secondary reactions are depleting the initial reactants as well. Therefore, the measured rate constants may not be simple bimolecular rate constants, but are probably more complex apparent second order rate constants.

TABLE 1

A SUMMARY OF SOME RATE CONSTANTS
FOR SOME OZONE-OLEFIN REACTIONS

Initial Reactant Concentrations (moles/ℓ)		Reported Rate Constants ($\ell mole^{-1} sec^{-1}$)
$(olefin)_0$	$(O_3)_0$	
	(Ethylene)	
$\sim 3 \times 10^{-7}$	$\sim 1 \times 10^{-7}$	1.6×10^3
$\sim 5 \times 10^{-7}$	$\sim 5 \times 10^{-7}$	0.9×10^3
$\sim 8 \times 10^{-7}$	$\sim 8 \times 10^{-7}$	0.78×10^3
$\sim 1 \times 10^{-4}$	$\sim 2 \times 10^{-4}$	1.8×10^3
$\sim 1 \times 10^{-3}$	$\sim 2 \times 10^{-4}$	2.4×10^3
$\sim 1 \times 10^{-3}$	$\sim 2 \times 10^{-4}$	1.6×10^3
	(Propene)	
$\sim 3 \times 10^{-7}$	$\sim 5 \times 10^{-8}$	3.7×10^3
$\sim 5 \times 10^{-7}$	$\sim 5 \times 10^{-7}$	8×10^3
$\sim 2 \times 10^{-6}$	$\sim 3 \times 10^{-7}$	4.8×10^3
$\sim 1 \times 10^{-3}$	$\sim 2 \times 10^{-4}$	6.7×10^3
$\sim 1 \times 10^{-3}$	$\sim 2 \times 10^{-4}$	6.4×10^3
$\sim 1 \times 10^{-3}$	$\sim 2 \times 10^{-4}$	5.5×10^3
	(Trans-2-butene)	
1×10^{-8}	1×10^{-8}	2.6×10^5
$\sim 2 \times 10^{-8}$	$\sim 2 \times 10^{-8}$	1.6×10^5
$\sim 1 \times 10^{-3}$	$\sim 2 \times 10^{-4}$	$2. \times 10^4$
	(Cis-2-butene)	
$\sim 4 \times 10^{-8}$	$\sim 4 \times 10^{-8}$	$2. \times 10^5$
$\sim 1 \times 10^{-3}$	$\sim 2 \times 10^{-4}$	1.3×10^4
	(1-Butene)	
$\sim 4 \times 10^{-8}$	$\sim 4 \times 10^{-8}$	6×10^3
$\sim 1 \times 10^{-3}$	$\sim 2 \times 10^{-4}$	4×10^3
	Methylpropene	
$\sim 4 \times 10^{-8}$	$\sim 4 \times 10^{-8}$	1.4×10^4
$\sim 1 \times 10^{-3}$	$\sim 2 \times 10^{-4}$	3.6×10^4

The ozone olefin reactions studied followed second order kinetics and the apparent second order rate constants were determined and are summarized in Table 2.

TABLE 2

A SUMMARY OF THE RATE CONSTANTS FOR OZONE-OLEFIN REACTIONS AS DETERMINED IN THIS STUDY

Initial Reactant Concentration (moles/ℓ)		Value of the Rate Constant ($\ell mole^{-1} sec^{-1}$)
$(olefin)_o$	$(O_3)_o$	
	Ethylene + Ozone	
5×10^{-5}	1×10^{-5}	0.8×10^3
1×10^{-5}	0.3×10^{-5}	0.9×10^3
0.1×10^{-5}	0.1×10^{-5}	1.5×10^3
	Propene + Ozone	
5×10^{-5}	1×10^{-5}	5×10^3
3×10^{-5}	1×10^{-5}	6×10^3
1×10^{-5}	0.75×10^{-5}	7×10^3
	1-Butene + Ozone	
4×10^{-5}	1×10^{-5}	6×10^3
1×10^{-5}	0.1×10^{-5}	6×10^3
0.1×10^{-5}	0.1×10^{-5}	7×10^3
	Methylpropene + Ozone	
5×10^{-5}	1×10^{-5}	8×10^3
2×10^{-5}	1×10^{-5}	10×10^3
1×10^{-5}	1×10^{-5}	8×10^3
	Trans-2-butene + Ozone	
$.16 \times 10^{-5}$	$.06 \times 10^{-5}$	85×10^3
0.1×10^{-5}	0.1×10^{-5}	120×10^3
	Cis-2-butene + Ozone	
0.2×10^{-5}	0.1×10^{-5}	73×10^3
0.04×10^{-5}	0.04×10^{-5}	130×10^3

For olefins other than methylpropene the values of the apparent second order rate constants appear to increase as the initial concentration of olefin is decreased, which again suggests that the measured rate constant is not a simple bimolecular rate constant for the olefin-ozone reaction. Formation of significant amounts of aerosol in the reaction of cis or trans-2-butene at concentrations of olefin greater than about 0.5×10^{-5} mole/ℓ prevented accurate determination of the rate constants at olefin concentrations higher than 0.5×10^{-5} mole/ℓ. It is thought that the formation of aerosols produces complications at concentrations of olefins greater than 5×10^{-6} mole/ℓ in the measurements of the rate constants for the cis and trans-2-butene and may be the reason for the discrepancies in the reported values of the rate constants for these two olefins.

Aerosols were generated in the reactions with ozone of each of the olefins studied. The intensity of scattered light as a function of olefin concentration and reaction time were measured for trans-2-butene and ethylene. An induction period between the time the reaction is started and the first scattered light can be measured was observed for both olefins. This induction period is a strong function of the concentration of olefin as is also the maximum intensity of scattered light.

Future experiments using the stopped-flow method should include:

1. Rate measurements down to about 5×10^{-8} mole/ℓ concentrations using a longer path length cell
2. Careful measurement to determine the effect or O_2 concentration on the apparent rate constants and reaction stoichiometry
3. Determination of the product distribution in the cis and trans-2-butene reactions at high (c.a. $\sim 10^{-4}$ mole/ℓ) and low (c.a. $\sim 10^{-7}$ mole/ℓ) concentrations
4. Characterization of aerosol composition.

SECTION II

EXPERIMENTAL METHODS

This investigation was initiated in order to resolve the discrepancies in the published values of the second order rate constants for ozone-olefin reactions. Rate constants were to be measured over large concentration ranges of reactants using the same experimental method.

The experimental apparatus for measurement of reaction rates is shown in Figure 1. Figure 2 shows the reaction cell which is constructed of Pyrex glass, except for the front and rear windows which are of quartz. The quartz windows are joined to the Pyrex cell with a small amount of Torr Seal cement. The four-way valve is also Pyrex and is lubricated with a small amount of silicone stopcock grease.

Gas flows were measured with rotameters which were previously calibrated using either a wet test meter or a soap bubble meter. The calibration curve for the 1% (by volume) olefin in nitrogen mixture was assumed to be the same as the calibration curve for pure N_2. Some typical gas flows in an experiment would be 35 liters/minute for N_2, 0.15 liter/minute for the $O_2 + O_3$ mixture, and 0.10 liter/minute for the 1% olefin in N_2 mixture. By adjusting the flow rates the concentrations of the olefin and O_3 could be varied. Conditions for turbulent flow of gases, which should facilitate mixing of the reactant gases, existed in the 4 mm I.D. tubing that leads to the reaction vessel. Typical total pressures in the reaction cell are 770 torr to 800 torr.

The photometric system for measuring the ozone concentration consisted of a low pressure Hg lamp (Pen Ray), an adjustable slit, two quartz lenses about 2 focal lengths apart to collimate the light beam, another slit, the quartz

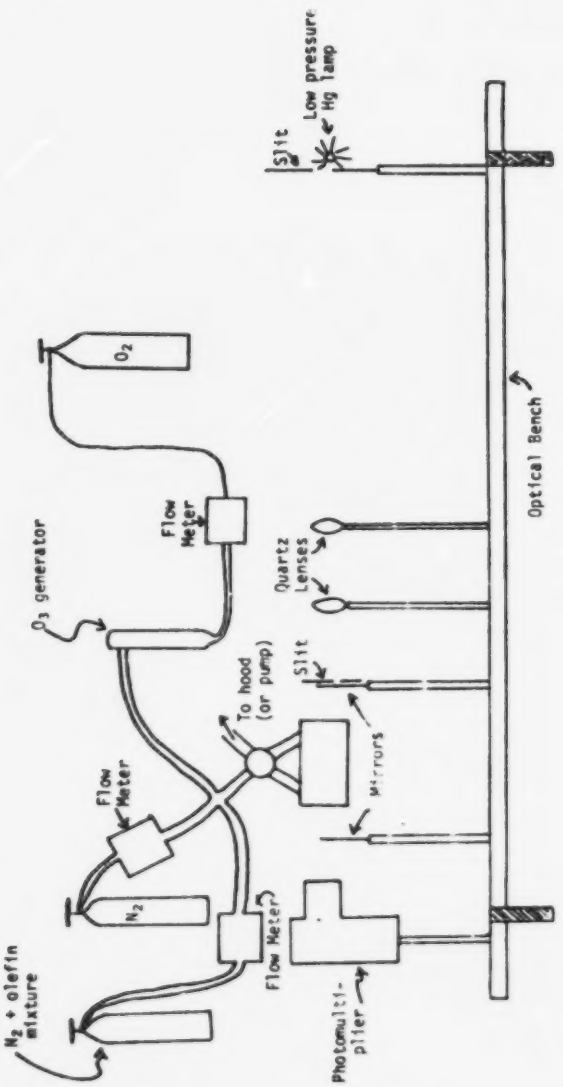

Figure 1. Schematic of Apparatus

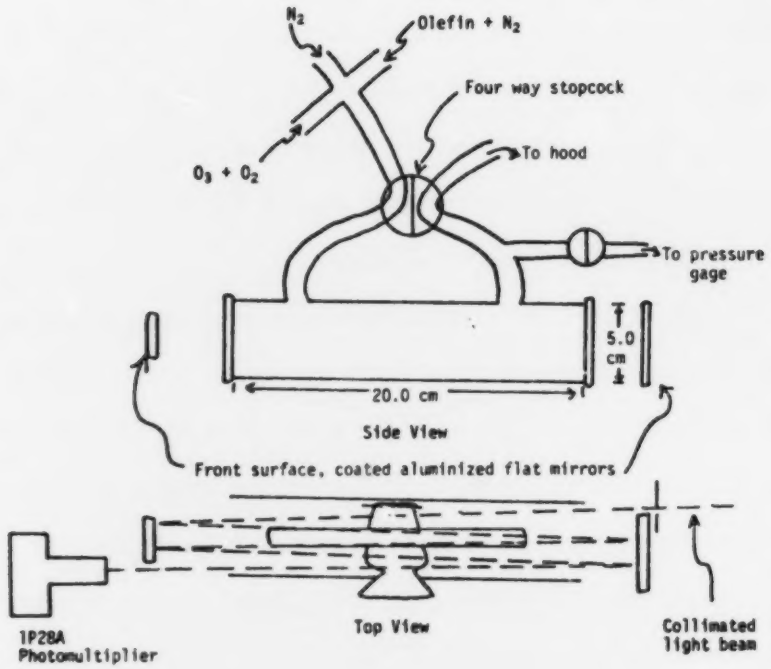

Figure 2. Diagram of Reaction Cell

windows of the cell, two front surfaced aluminized mirrors, an interference filter, and finally a RCA 1P28A photomultiplier tube. With the aid of a He-Ne laser the mirrors could be adjusted to give either 1, 3, or 5 traverses through the cell so that a light path length of 100. cm could easily be attained with the 20 cm long cell. The photomultiplier was housed in a box designed such that the only light which could strike the photocathode was the light which passed through the interference filter. The filter has a maximum of 15% transmission at 2500 A and a one half band width of 125 A. Signal from stray light other than that of about 2500 A amounted to no more than 0.5% of the total signal measured. The Hg resonance line emission at 2537 A is at a well-defined wavelength and the light intensity measured with the photomultiplier should be monochromatic light at 2537 A wavelength.

The current generated by the photomultiplier passed through a load resistor. The voltage drop across this resistor was measured with a potentiometric strip chart recorder. Conditions in the photomultiplier circuit were such that the current going through the load resistor was much less than 1% of the current going through the dynode voltage divider circuit. Therefore the photocurrent generated should be directly proportional to the light intensity striking the photocathode.

The ozone generator was constructed from two concentric glass tubes. The inner tube contained an electrolyte (6 N H_2SO_4) and the outer tube was covered with metal foil and insulated. Oxygen gas flowed between the tubes and a voltage of about 15,000 volts was applied between the tubes to generate sufficient quantities of ozone for the experiments. After allowing for a half-hour warm up, the O_3 concentration in the effluent O_3 - O_2 mixture was quite constant and changed no more than ±2% within a time interval of two hours.

In a typical experiment the gas flow rates are adjusted to the desired values with the four-way stopcock turned such that the mixed gases flow through

the reaction cell. After about two minutes the ozone concentration reaches a steady state (as measured photometrically). Ther the flow through the cell is stopped by rotation of the four-way valve. Pressure inside the cell is measured with a mercury free diaphragm gage. The percent transmission of the reaction mixture is then measured as a function of time with the strip chart recorder. Ozone concentrations at different reaction times can be easily calculated from the optical density (or absorbance).

The extinction coefficient of O_3 at 2537 A (ε) was determined using three traversals of light and five traversals of light through the reaction cell. By passing the ozonized oxygen at a known flow rate through a KI trap and then titrating the triiodide ion generated with standardized sodium thiosulfate, it was possible to calculate the concentration of O_3 in the oxygen. A typical concentration of O_3 in the O_2 would be between 1 and 5 x 10^{-4} moles/liter. The concentration in the O_2 could be varied by changing the voltage on the primary of the ozonizer transformer. The ozonized oxygen stream was diluted in the mixing chamber with nitrogen gas. By knowing the flow rates of the ozonized oxygen and the diluting nitrogen the concentration of O_3 in the cell could be calculated. The photometric measurement of I/I_0, where I is the light intensity passing through the cell with the O_3, O_2, N_2 mixture in the cell and I_0 is the light intensity getting through the cell with no O_3 present, permits the value of ε in Equation I to be calculated.

$$\log_{10}\left(\frac{I_0}{I}\right) = \varepsilon CI \qquad (I)$$

Quantities C and I are respectively the reaction cell ozone concentration in moles per liter, and the path length of the cell. The extinction coefficient ε was calculated to be 2755± 100 liter $mole^{-1}cm^{-1}$. This value is in excellent agreement with the value determined by Johnston at 2537 A (5). Equation (I)

was obeyed to the limits of photometric accuracy and the accuracy to which the gas flow rates could be measured. The combined error would be about 5%.

To determine the stoichiometry of ozone-olefin reactions, the ozone concentration was measured photometrically as already described and the olefin concentration was measured using a Varian Model 600 D gas chromatograph equipped with a flame ionization detector and a 5% SE-30 on Chromasorb P 100/120 mesh 6 ft. long 1/8 in. diameter copper column. The gas chromatograph was calibrated using olefin-N_2 gas mixtures of known composition. By measuring the ozone and olefin concentration before and after completion of the chemical reaction, the amounts of each reactant consumed by the reaction could be calculated.

Scattered light intensities produced by aerosols were measured by using the beam (6328 A wavelength) from a 0.5 mw He-Ne laser directed along a path roughly parallel to the longitudinal axis of the cylindrical reaction vessel. An RCA 1P22 photomultiplier tube was mounted perpendicular to the laser beam and was used to moniter the intensity of the scattered laser light as a function of time. To ensure that the light being measured by the 1P22 photomultiplier was the same wavelength as the light incident on the cell, a blackened box was built around the reaction vessel, and an interference filter with a half band width of 100 Å at 6328 Å was placed between the photomultiplier and the reaction vessel. (To further minimize interference from stray light, the scattering measurements were done in a dark room.) The signal from the photomultiplier was amplified with a Gencom Model 1012 picoammeter and the voltage output was measured with a stripchart recorder.

All olefins used were Matheson C.P. grade gases which were no less than 99.0% pure. Matheson high purity nitrogen (99.99%) was used in the preparation of the gas mixtures and for the diluting gas in the stopped flow experiments. Ozone was generated by passing Matheson Extra Dry (99.6%) oxygen through the ozonizer.

SECTION III

RESULTS AND DISCUSSION

1. Stoichiometry of some ozone-olefin reactions

The values of moles olefin used/moles ozone used, symbolized by the letter "n", are compiled for some olefins in Table 3. The stoichiometric determinations were made with a 1.0 cm diameter by 20.0 cm long Pyrex reaction cell with quartz windows fastened on each end with Varian Torr Seal epoxy. Typical experimental conditions were:

gas	gas flow rate (/min)
1% olefin in N_2	0.8
1% O_3 in O_2	0.6
N_2	8.

Temperature = 25 ± 2°C

Total gas pressure in cell = 770 torr

The symbols $(olefin)_o$ and $(O_3)_o$ refer to the initial olefin and ozone concentrations respectively. Both concentrations are expressed in moles/liter.

TABLE 3

THE STOICHIOMETRY OF SOME OZONE-OLEFIN REACTIONS

Ethylene + Ozone

$(Olefin)_o \times 10^5$	$(O_3)_o \times 10^5$	$(Olefin)_o/(O_3)_o$	n
0.775	1.32	0.59	0.84
2.39	1.30	1.84	1.00
4.00	1.25	3.20	1.25
3.55	1.20	2.96	1.20
5.35	1.17	4.57	1.28

Propene + Ozone

$(Olefin)_o \times 10^5$	$(O_3)_o \times 10^5$	$(Olefin)_o/(O_3)_o$	n
2.04	2.08	0.981	1.15
1.41	2.21	0.516	1.16
1.56	2.11	0.739	1.16
2.36	2.04	1.16	1.20
0.712	0.897	0.794	0.961
0.353	1.03	0.343	0.944
0.353	0.987	0.358	0.98
0.579	1.41	0.410	1.20
0.574	1.42	0.410	1.22
1.33	1.36	0.979	1.15
0.952	1.37	0.695	1.21
0.433	1.45	0.30	0.98
0.615	1.42	0.433	1.06
1.17	1.39	0.842	1.06
0.421	1.47	0.286	0.93
1.13	1.39	0.813	1.11
1.36	2.10	0.648	1.12
0.944	2.30	0.411	1.10
1.41	2.01	0.704	1.22
1.87	2.05	0.91	1.19
0.747	1.85	0.404	1.05
4.75	1.20	3.96	1.08
3.42	1.21	2.83	1.13
1.69	1.31	1.29	1.06
4.18	1.22	3.43	1.23

TABLE 3. Cont.

1-Butene + Ozone

$(Olefin)_o \times 10^5$	$(O_3)_o \times 10^5$	$(Olefin_c/(O_3)_o$	n
2.06	2.06	1.00	1.14
1.01	1.37	0.737	1.13
1.39	1.38	1.01	1.22
1.27	1.36	0.930	1.10
0.767	1.36	0.564	1.13
0.385	1.41	0.273	1.01
2.47	1.15	2.15	1.18
2.47	1.25	1.98	1.03
2.47	1.21	2.04	1.13
1.86	1.25	1.49	1.07
3.92	1.13	3.47	1.23
5.46	1.12	4.88	1.39
2.82	1.28	2.20	1.09
5.46	1.07	5.10	1.28
5.46	1.12	4.88	1.37
0.297	1.34	0.222	1.01

Cis-2-Butene + Ozone

$(C_4H_8) \times 10^5$	$(O_3) \times 10^5$	$(C_4H_8)_o/(O_3)_o$	n
3.84	1.20	3.2	0.91
3.63	1.30	2.79	0.91
2.21	1.29	1.71	1.09
5.30	1.24	4.27	1.12
5.09	1.19	4.28	1.15
0.068	0.089	0.77	1.2
0.039	0.040	1.0	1.0
0.037	0.054	0.67	0.9
0.037	0.10	0.37	0.7

Methyl Propene + Ozone

$(Olefin)_o \times 10^5$	$(O_3)_o \times 10^5$	$(Olefin)_o/(O_3)_o$	n
4.21	1.19	3.54	1.82
2.83	1.21	2.34	1.68
5.70	1.13	5.04	1.97
1.34	1.37	0.978	1.53
1.93	1.36	1.42	1.58
2.23	1.99	1.12	1.55
3.10	2.11	1.47	1.61
1.60	1.56	1.03	1.37
1.35	1.56	0.864	1.44
2.19	1.50	1.46	1.52
2.50	2.11	1.18	1.46
1.36	2.08	0.654	1.53
2.75	2.00	1.38	1.62

The last four determinations for cis-2-butene in Table 3 were made with the 5.0 cm diameter by 20.0 cm long cell with an N_2 flow of about 35 ℓ/min, and an ozonized oxygen flow of about 0.2 ℓ/min.

Figures 3 through 7 are graphs of the value of n plotted as a function of the ratio of $(olefin)_o/(O_3)_o$ for each of the olefins listed in Table 1. The graphs for ethylene, 1-butene, and methylpropene indicate that the value of n for the chemical reaction increases as the ratio of $(olefin)_o/(O_3)_o$ increases. Similar trends for cis-2-butene and propene may also exist but are not as pronounced as shown in Figures 4 and 6, although a slight decrease in n at smaller values of $(olefin)_o/(O_3)_o$ should be noted. Each of the values of n are subject to approximately $\pm$ 10% relative error.

An increase in the value of n with increasing $(olefin)_o/(O_3)_o$ may be due to some reactive intermediate (or product) reacting with either the olefin or with ozone. The sequence of reactions shown below may qualitatively account for the trend in n with respect to $(olefin)_o/(O_3)_o$:

$$\text{olefin} + O_3 \longrightarrow \text{olefin} \cdot O_3 \qquad (1)$$

$$\text{olefin} \cdot O_3 \longrightarrow \text{stable products} \qquad (2)$$

$$\text{olefin} \cdot O_3 \longrightarrow X \qquad (3)$$

$$X + \text{olefin} \longrightarrow Y \qquad (4)$$

$$X + O_3 \longrightarrow Z \qquad (5)$$

The species olefin $\cdot$ O_3 is assumed to be an ozone olefin adduct, perhaps a 1,2,3-trioxolane, which contains excess energy. The lifetime of such an intermediate formed in the reaction of cis-2-butene and ozone may have up to 45 kcal/mole excess energy and a lifetime of about 10^{-11} sec [1]. It has been postulated that the olefin $\cdot$ O_3 adduct can decompose to give HCO, C_3H_7, C_2H_5 and CH_3CO free radicals in the case of the ozone + cis-2-butene reaction, CH_3CO with the ozone + ethylene reaction, and perhaps C_3H_7 in ozone + methylpropene. These free radicals have been detected by means of a photoionization mass spectrometer [1]. Formation of free radicals is represented

collectively by reaction (3). Such free radicals can presumably react directly with the olefin or ozone, giving rise to the observed dependence of stoichiometry on the initial ratio of $(\text{olefin})_o/(O_3)_c$. Molecular oxygen was also present in these stoichiometric determinations. (The partial pressure of O_2 in the experiments done with the 1.0 cm by 20 cm cell was about 50 torr.) Free radicals are known to react with molecular oxygen to produce yet another generation of radicals capable of destroying either olefin or ozone. In summary, the fact that the stoichiometry for the reactions of the olefins described from 1:1 and the observed dependence of n on the ratio of $(\text{olefin})_o/(O_3)_o$ both suggest that the reaction is most certainly not a simple bimolecular reaction between ozone and olefin. A rate constant determined from the measured decay rate of ozone or olefin should be considered an "apparent rate constant" and not a "bimolecular rate constant" for the ozone-olefin reaction.

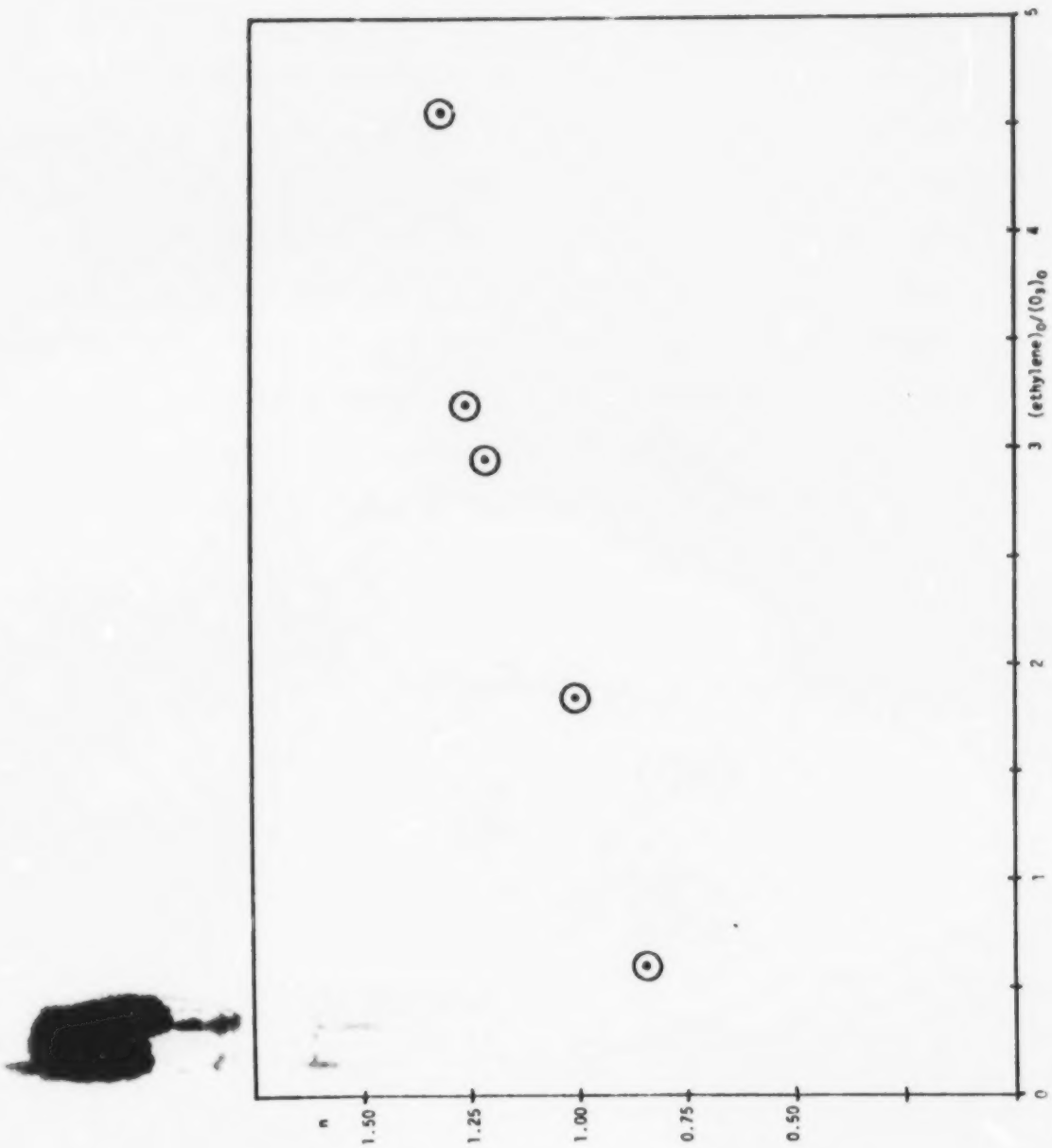

Figure 3. n vs. (ethylene)$_0$/(O$_3$)$_0$

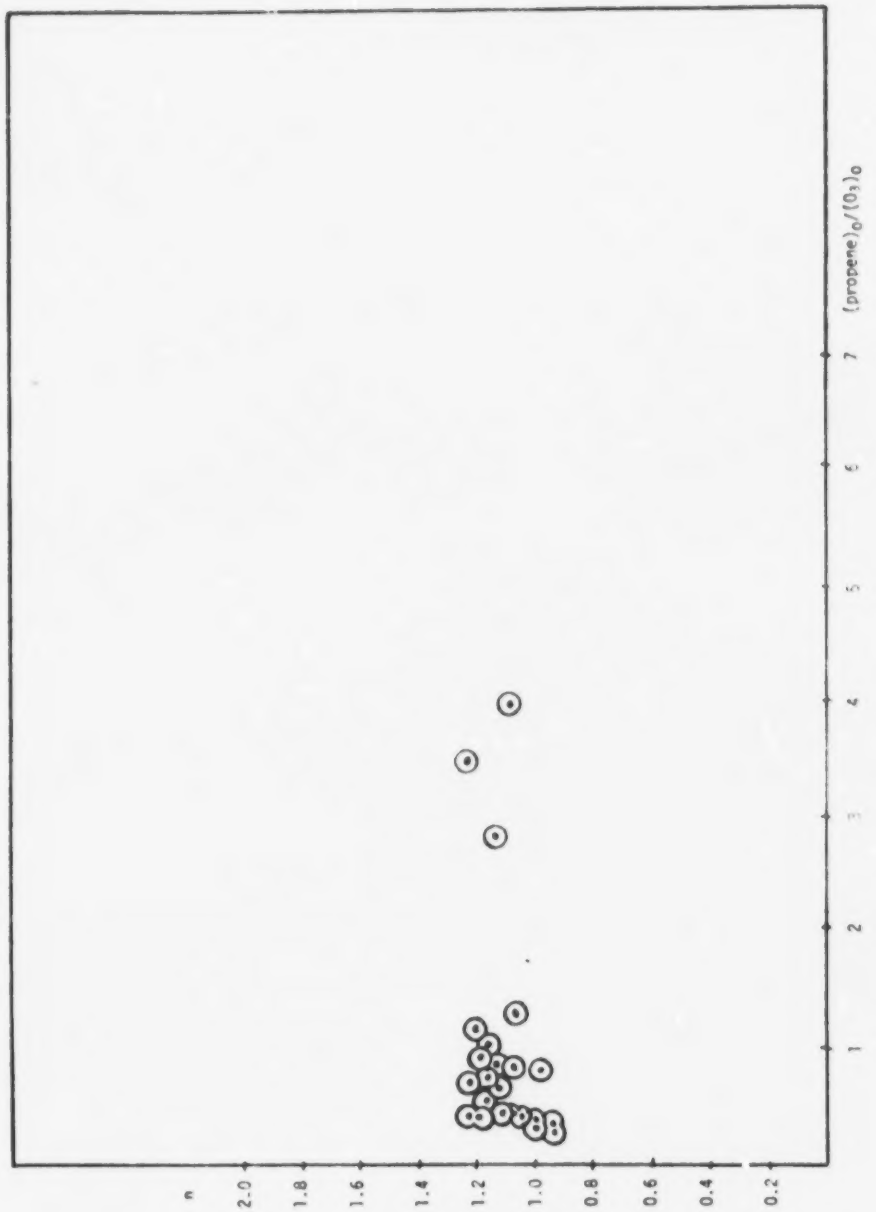

Figure 4. n vs. (propene)$_0$/(O$_3$)$_0$

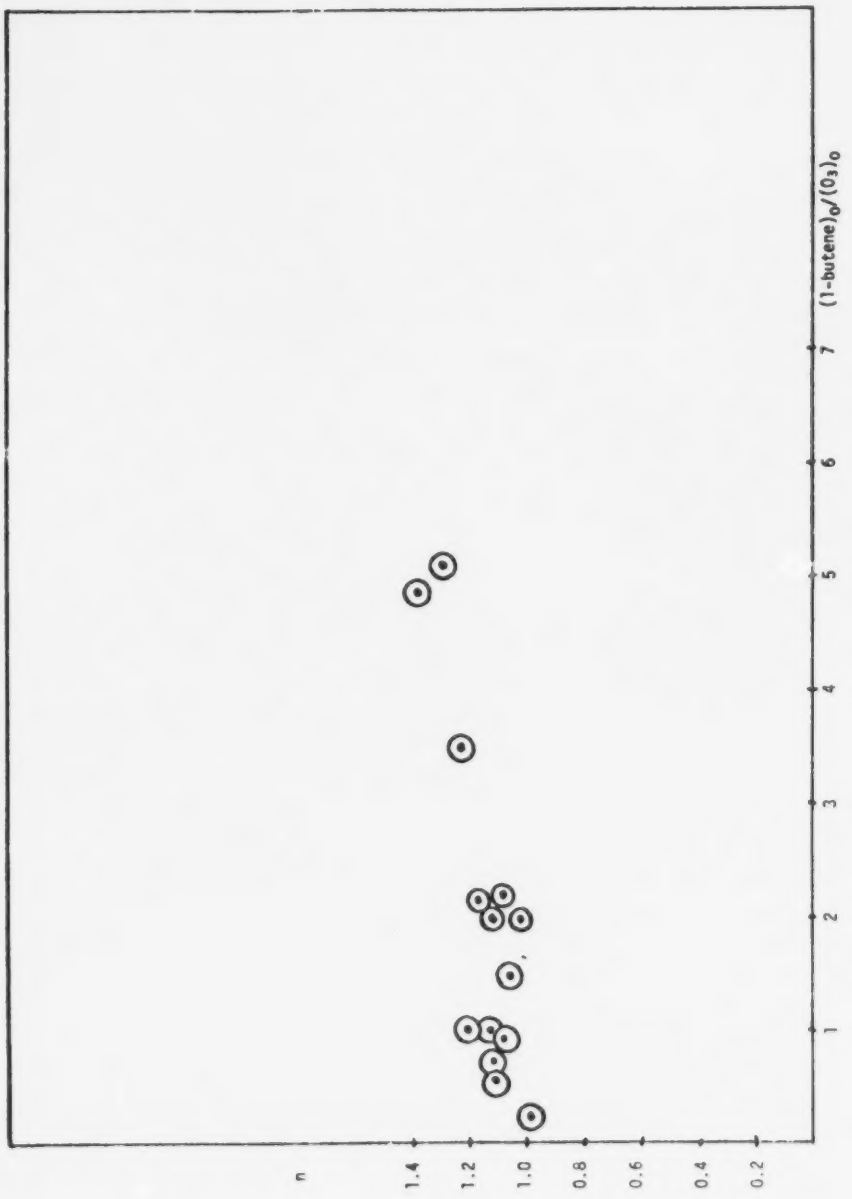

Figure 5. n vs. (1-butene)$_0$/(O$_3$)$_0$

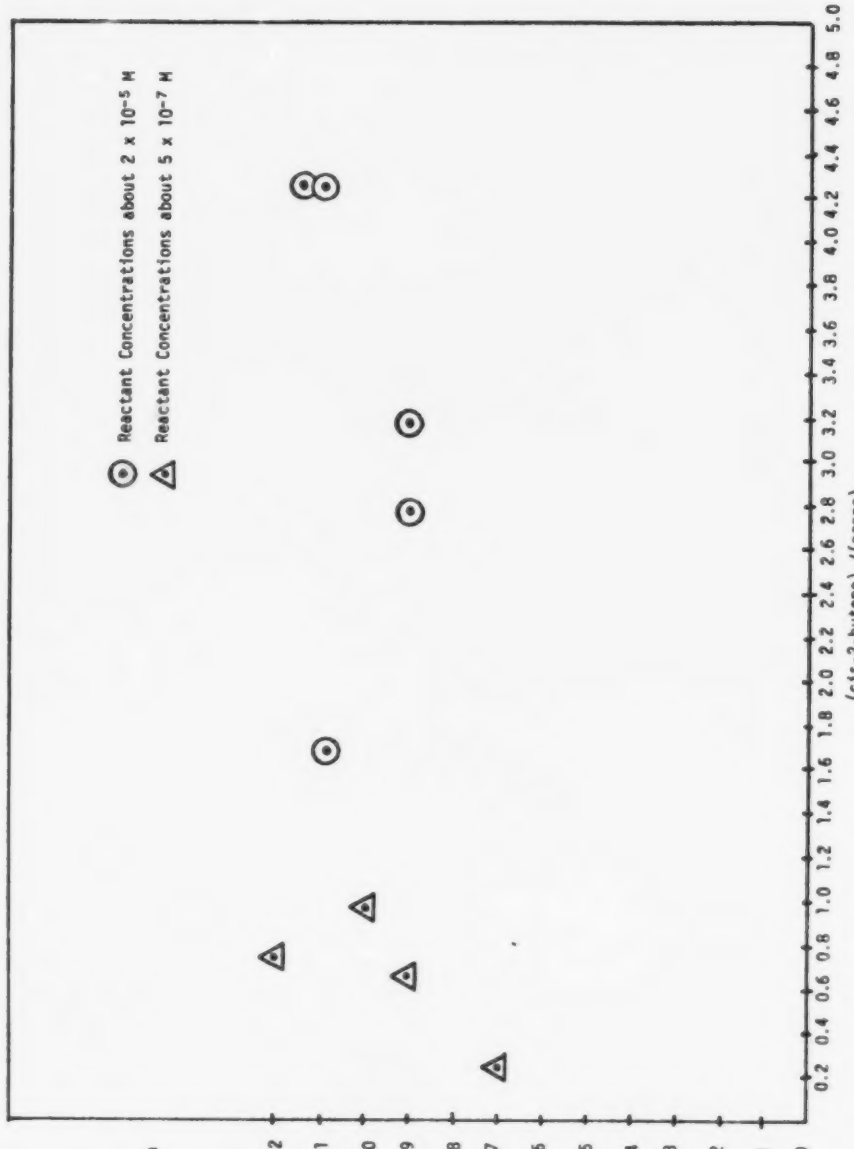

Figure 6. n vs. (cis-2-butene)$_0$/(O_3)$_0$

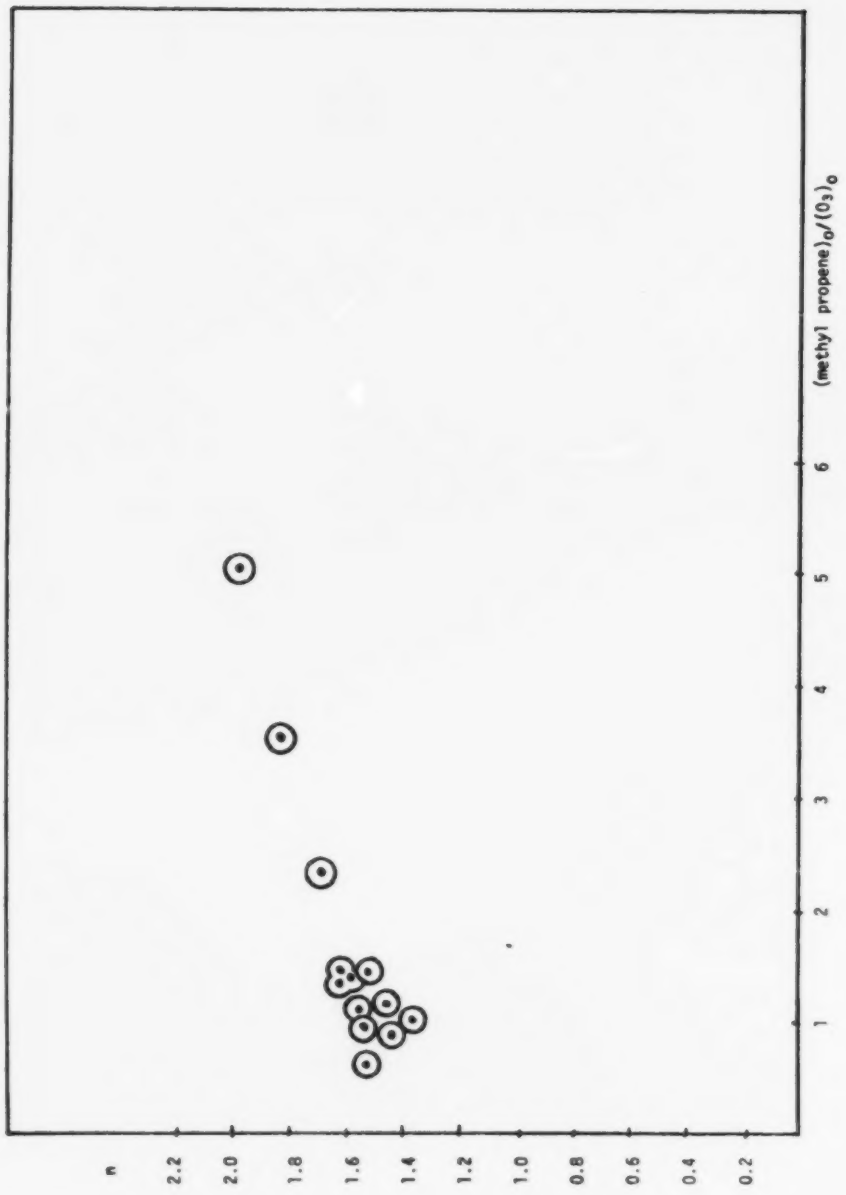

Figure 7. n vs. (methyl propene)$_0$/(O$_3$)$_0$

2. Rates of ozone-olefin reactions

Previous measurements of rates of ozone-olefin reactions have shown that the chemical reaction appears to be first order in ozone, first order in olefin and second order overall [2, 3, 4, 7]. The ozone concentration was determined photometrically as described in the "Experimental Methods" section and the olefin,concentration, symbolized by (olefin), at any elapsed reaction time "t" (in seconds) was calculated from Equation (II):

$$(\text{olefin}) = (\text{olefin})_0 - n\Delta(O_3) \qquad \text{(II)}$$

where n = moles olefin consumed/moles ozone consumed, $\Delta(O_3)$ = initial concentration of ozone in moles/liter minus the concentration of ozone at elapsed reaction time t, and $(\text{olefin})_0$ = initial concentration of olefin in moles/liter. When necessary, correction for the absorbtion of the 2537 A analyzing light by products was made by calculating the ozone concentration at elapsed time t, symbolized by (O_3), from the expression:

$$(O_3) = (O_3)_0 \left[\frac{At - A\infty}{A_0 - A\infty} \right] \qquad \text{(III)}$$

where At = absorbance at elapsed reaction time t, A_0 = initial absorbance, $A\infty$ = absorbance after approximately eight reaction half lives have elapsed, and $(O_3)_0$ = initial ozone concentration. Absorbance (or optical density), as used here, is equal to $\log \left(\frac{I_0}{I} \right)$, where I and I_0 are transmitted light intensities with and without ozone in the reaction vessel. Values of $A\infty$ for ethylene, propene, 1-butene, and methylpropene did not exceed 0.02.

The integrated form of the second order rate equation:

$$\log \left\{ \frac{(O_3)_0}{(\text{olefin})_0} \times \frac{(\text{olefin})}{(O_3)} \right\} = \frac{[(\text{olefin})_0 - n(O_3)_0]kt}{2.30} \qquad \text{(IV)}$$

was used to evaluate the value of the apparent second order rate constant,

symbolized by k, for the various olefins.

Figures 8 through 11 show the left hand side of Equation (IV), which is symbolized by f, plotted on the log scale as a function of time in seconds (t) for ethylene, propylene, 1-butene, and methylpropene. The linearity of the graphs suggests that these ozone olefin reactions appear to be second order overall.

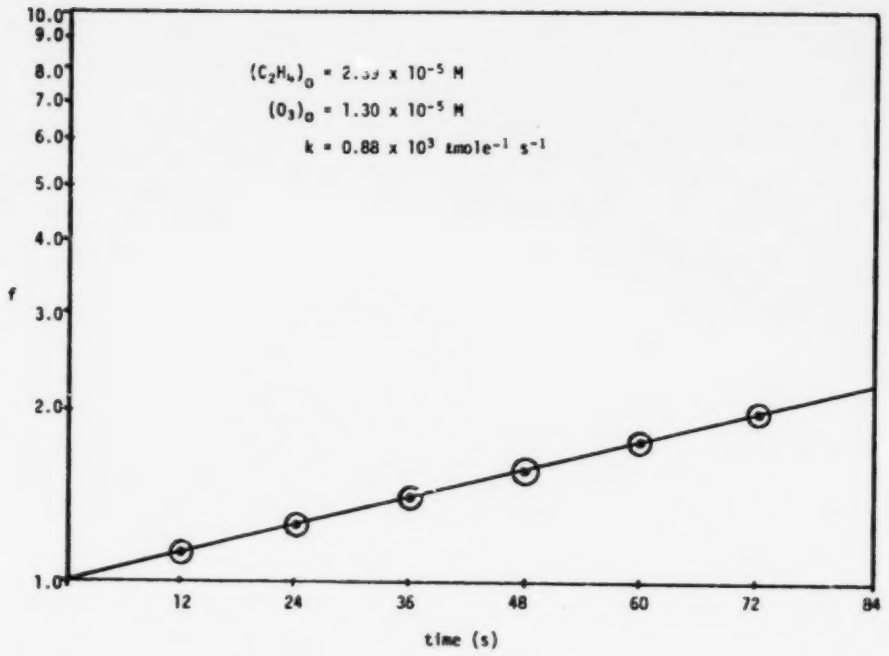

Figure 8. Second Order Plot. Ethylene + Ozone.

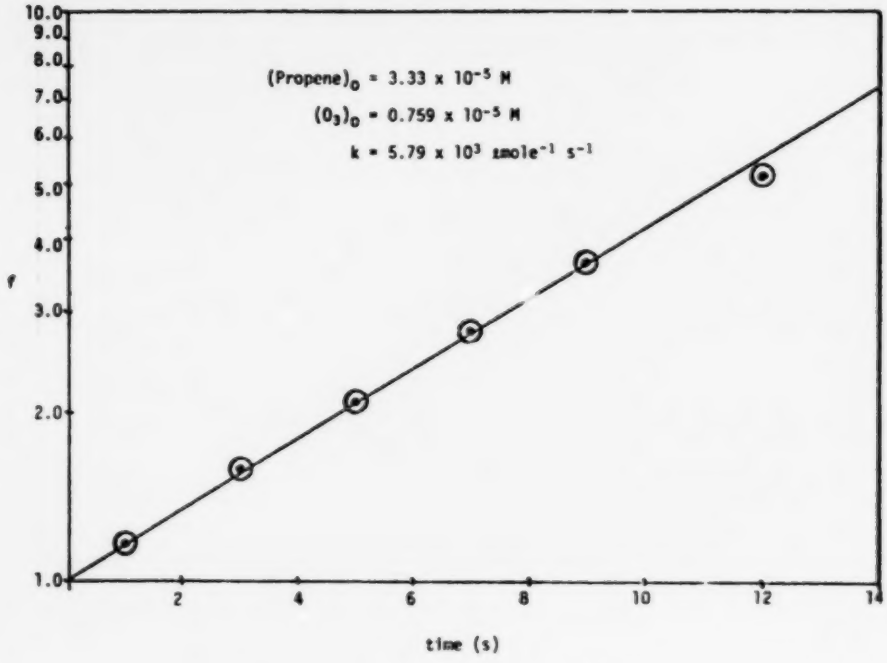

Figure 9. Second Order Plot. Propene + Ozone.

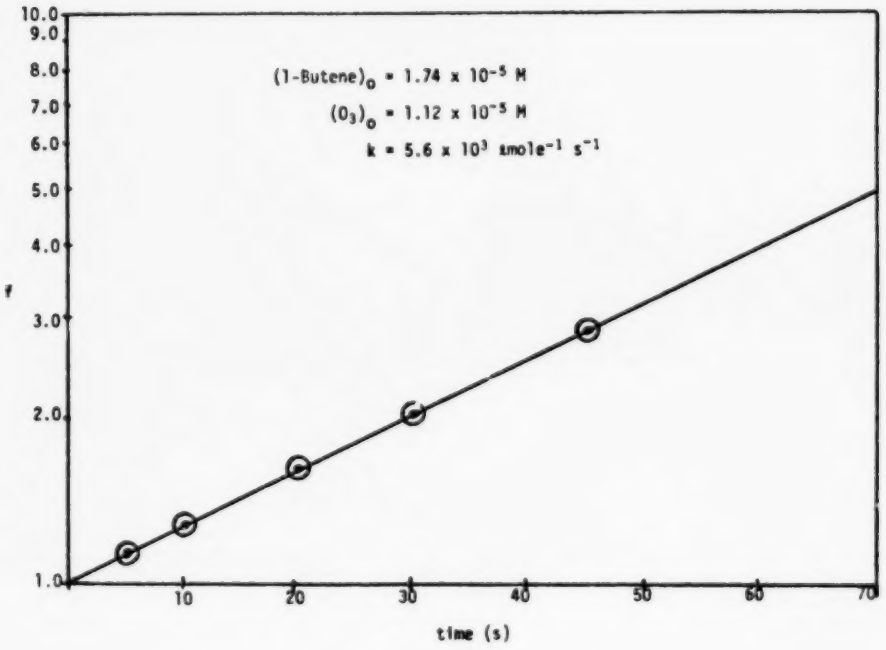

Figure 10. Second Order Plot. 1-Butene + Ozone.

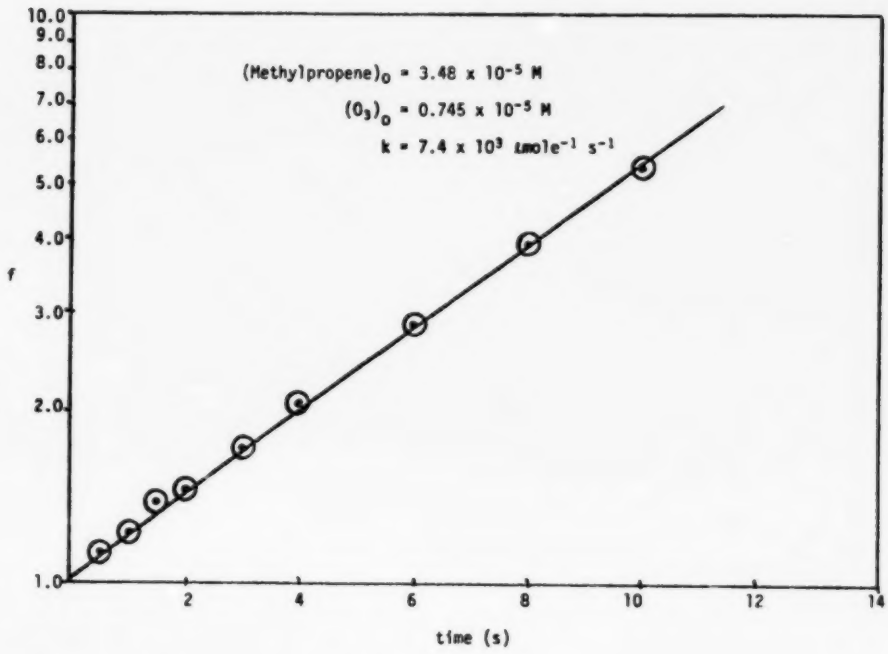

Figure 11. Second Order Plot. Methylpropene + Ozone.

Table 4 is a summary of the apparent second order rate constants as determined by the methods stated above. The units of k are liters $mole^{-1}sec^{-1}$. $(Olefin)_o$ and $(O_3)_o$ are initial concentrations of olefin and ozone respectively in moles/liter.

TABLE 4

APPARENT SECOND ORDER RATE CONSTANTS
FOR SOME OZONE-OLEFIN REACTIONS

Ethylene + Ozone

Experiment	$(C_2H_4)_o x10^5$	$(O_3)_o x10^5$	Apparent 2nd Order Rate Constant x 10^{-3}
1	5.35	1.17	0.78
2	3.55	1.20	0.76
3	1.25	1.25	0.90
4	2.39	1.30	0.88
5	0.775	1.32	1.0
6	1.87	0.310	0.916
7	1.82	0.320	0.905
8	1.73	0.345	0.923
9	1.63	0.324	0.963
10	1.48	0.324	0.927
11	1.46	0.310	0.919
12	1.02	0.612	0.813
13	0.977	0.579	1.13
14	0.699	0.445	0.969
15	0.677	0.443	0.849
16	0.670	0.460	1.09
17	0.654	0.432	1.20
18	0.60	0.0749	0.92
19	0.484	0.349	1.12
20	0.478	0.325	1.06
21	0.47	0.0667	0.98
22	0.38	0.0710	0.88
23	0.112	0.0787	1.5
24	0.112	0.0814	1.6

Propene + Ozone

	$(C_3H_6)_o x10^5$	$(O_3)_o x10^5$	Apparent 2nd Order Rate Constant x 10^{-3}
25	5.32	1.00	4.89
26	3.33	0.759	5.79
27	2.05	1.04	5.66
28	1.83	0.761	5.96
29	1.00	0.750	7.3
30	1.05	0.489	5.63
31	1.34	0.454	5.79

TABLE 4 - Cont.

1-butene + Ozone

Experiment	$(1\text{-}C_4H_8)_o \times 10^5$	$(O_3)_o \times 10^5$	Apparent 2nd Order Rate A Constant x 10^{-3}
32	4.39	1.05	5.6
33	2.68	0.643	5.6
34	1.82	0.730	5.5
35	1.74	1.12	5.6
36	1.57	0.246	5.75
37	1.57	0.0623	6.13
38	1.55	0.138	6.2
39	1.55	0.0667	5.96
40	0.462	0.285	5.78
41	0.462	0.302	5.60
42	0.294	0.0765	6.19
43	0.196	0.0704	6.15
44	0.114	0.0820	6.2
45	0.113	0.0798	7.5
46	0.110	0.0781	7.4
47	0.105	0.0798	8.8
*48	0.10	0.10	7.6

*Plotted as $1/(O_3)$ vs. time.

Methylpropene + Ozone

	$(C_4H_8)_o \times 10^5$	$(O_3)_o \times 10^5$	Apparent 2nd Order Rate Constant x 10^{-3}
49	4.95	1.09	7.7
50	3.48	0.745	8.33
51	2.56	0.719	10.6
52	2.25	1.21	6.1
53	1.04	0.795	7.5

For experiments 1 through 5 in Table 4 the 1.0 cm diameter by 20.0 cm long reaction cell was used. The N_2 flow was about 8.0 ℓ/min, the ozone-oxygen mixture flow about 0.6 ℓ/min and the flow of the C_2H_4-N_2 mixture about 0.8 ℓ/min, although the flow rate of this mixture was varied to change $(C_2H_4)_o$. The total gas pressure was 795 ± 10 torr and the temperature of the reaction cell was 25 ± 2°C (room temperature).

Experiments 6 through 24 in Table 4 were carried out in the 5.0 cm diameter by 20.0 cm long reaction vessel. The N_2 flow was about 35. ℓ/min and the C_2H_4-N_2 flow rate was varied between about 0.1 and 1.5 ℓ/min. The

cell temperature was about 23 $\pm$ 2°C and the total gas pressure in the cell was about 790 $\pm$ 5 torr. For runs 18, 21, 22, the O_2 flow rate was 0.5 ℓ/min and for the other runs, 6 through 24, the O_2 flow rate was about 0.2 to 0.3 ℓ/min.

Experiments 25 through 29 were carried out in the 1.0 cm diameter by 20.0 cm long cell with conditions essentially the same as stated for runs 1 through 5. Experiments 30 and 31 were done in the 5.0 cm diameter by 20.0 cm long cell with conditions similar to those stated for experiments 6 through 24.

Experiments 32 through 35 were done in the 1.0 cm diameter by 20.0 cm long cell with conditions similar to those used for runs 1 through 5.

Experiments 36 through 48 were done in the 5.0 cm diameter by 20.0 cm long cell with conditions essentially the same as for runs 6 through 24. However, experiments 42 and 43 had an ozonized oxygen flow rate of about 0.4 ℓ/min whereas the other experiments had an ozonized oxygen flow rate of about 0.2 ℓ/min.

Since the stoichiometry in the reactions of ethylene, and 1-butene have not extensively been measured under the conditions stated for experiments 6 through 24 and 36 through 48 a stoichiometry of 1:1 has been used in the rate plots. It has been reported that the stoichiometric ratio n approaches 1 in pure N_2 for ozone-olefin reactions and seems to increase when O_2 is present [3, 8]. Since there is only about 1% O_2 in the gas mixtures in runs 6-24 and 36-48 the assumption of 1:1 stoichiometry is somewhat uncertain and should be measured more thoroughly over a range of $(\text{olefin})_o/(O_3)_o$. However, experiments done with a slight excess of O_3 with 1-butene and ethylene showed a stoichiometry of 1:1 with 1% O_2 in the gas mixture.

The data in Table 4 suggests that there may be a small increase in the value of k as the initial concentration of the olefin is decreased. In the case of ethylene k is about 0.8×10^3 ℓmole^{-1}sec^{-1} at $(C_2H_4)_o = 5 \times 10^{-5}$ mole/ℓ

and about 1.5×10^3 $\ell mole^{-1}sec^{-1}$ at $(C_2H_4)_o = 0.1 \times 10^{-5}$ mole/ℓ. For 1-butene k is about 5.6×10^3 $\ell mole^{-1}sec^{-1}$ at $(C_4H_8)_o = 4 \times 10^{-5}$ mole/ℓ and 8×10^3 $\ell mole^{-1}sec^{-1}$ at $(C_4H_8)_o = 0.1 \times 10^{-5}$ mole/ℓ. A similar trend is noted for the apparent second order rate constant of propene, although the trend is quite small and is not much larger than the experimental uncertainty of about 10%. The values for k in the propene reaction range from about 5×10^3 $\ell mole^{-1}$ sec^{-1} to about 7×10^3 $\ell mole^{-1}sec^{-1}$.

No trend in the value of k for methylpropene is detectable. The values of k range from 6×10^3 $\ell mole^{-1}sec^{-1}$ to 10×10^3 $\ell mole^{-1}sec^{-1}$. Measurements of k for methylpropene seem to show less reproducibility than for the other olefins shown in Table 4.

Results for trans-2-butene and cis-2-butene are shown in Table 5. The stoichiometry of the trans-2-butene-ozone reaction was only measured under conditions of a slight excess of O_3 with initial concentrations of O_3 and trans-2-butene of about 10^{-6} moles/ℓ, with the 5.0 cm diameter by 20.0 cm long cell and about 1% O_2 present at a temperature of 25°C. Under these conditions a value of $n = 1.35 \pm 0.1$ was determined for the trans-2-butene-ozone reaction.

TABLE 5

APPARENT SECOND ORDER RATE CONSTANTS FOR THE REACTION OF TRANS-2-BUTENE AND CIS-2-BUTENE WITH OZONE

Trans-2-butene + Ozone		
$(\text{Trans-2-butene})_o \times 10^5$	$(O_3)_o \times 10^5$	Apparent 2nd Order Rate Constant $\times 10^3 \ell\text{mole}^{-1}\text{sec}^{-1}$
0.097	0.116	150.
0.11	0.106	120.
0.12	0.113	80.
0.12	0.0814	100.
0.12	0.0781	90.
0.12	0.0814	86.
0.13	0.0858	121.
0.16	0.058	85.

Cis-2-butene + Ozone		
$(\text{Cis-2-butene}_o \times 10^5$	$(O_3)_o \times 10^5$	Apparent 2nd Order Rate Constant $\times 10^3$
0.23	0.124	73.
0.12	0.11	77.
0.71	0.089	75.
0.043	0.038	130.
0.041	0.034	140.
0.039	0.040	130.
0.037	0.054	120.
0.037	0.10	170.

Figures 12 and 13 show second order rate plots for trans and cis-2-butene respectively. The adherence to equation IV is fairly good for each of the olefins at olefin concentrations of 5×10^{-6} mole/ℓ or less. There may again be a slight tendency for the measured rate constant to increase as the olefin concentration is decreased, although such a conclusion is quite tenuous since the experimental uncertainty is probably on the order of $\pm$ 15% in both cases.

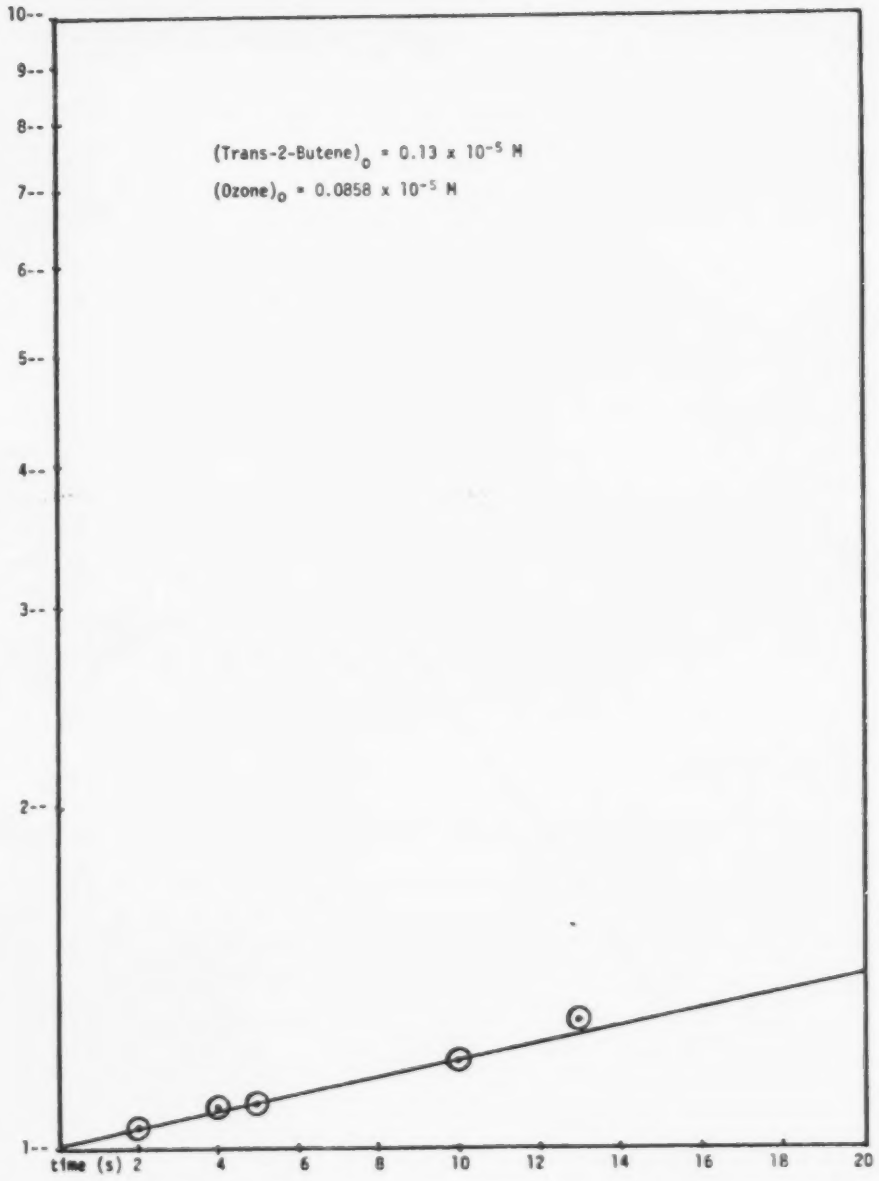

Figure 12. Second Order Plot. Trans-2-butene + Ozone.

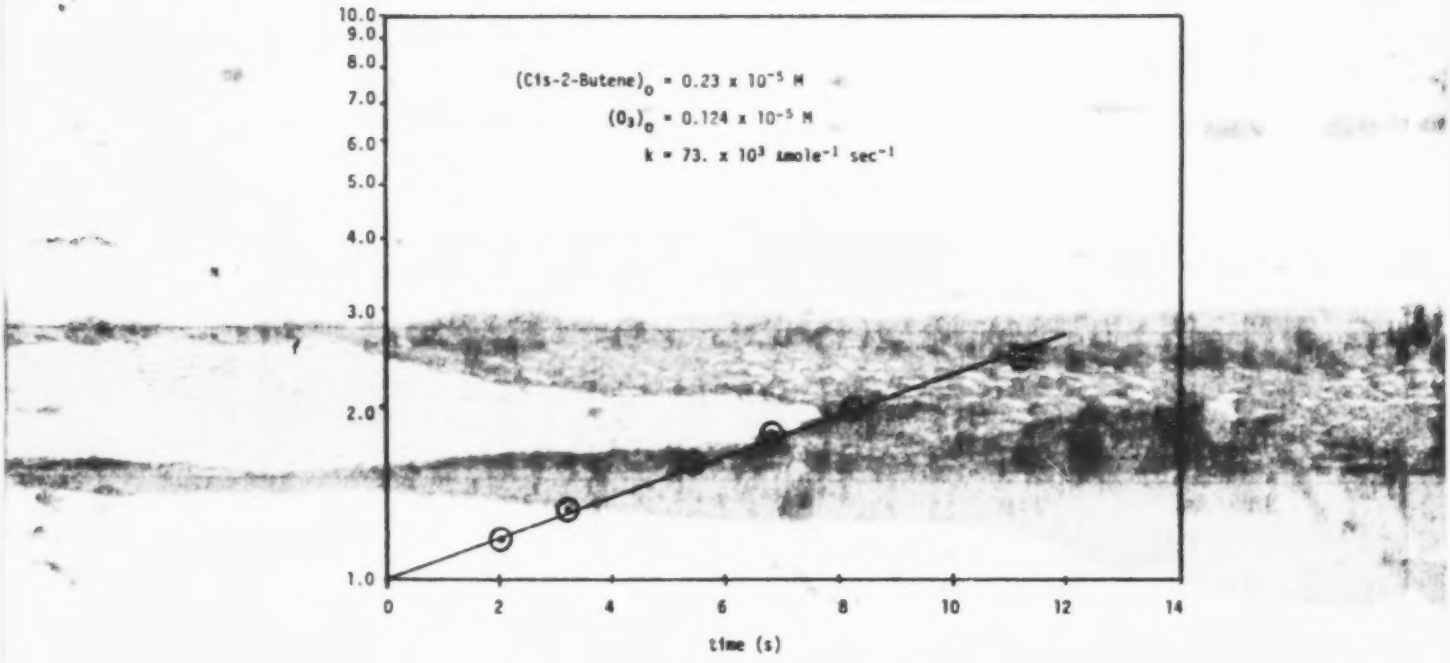

Figure 13. Second Order Plot. Cis-2-butene + Ozone.

When the initial concentration of either trans or cis-2-butene is increased beyond about 5×10^{-6}, large curvature is observed in the graph of f vs. time as shown in Figure 14 for trans-2-butene.

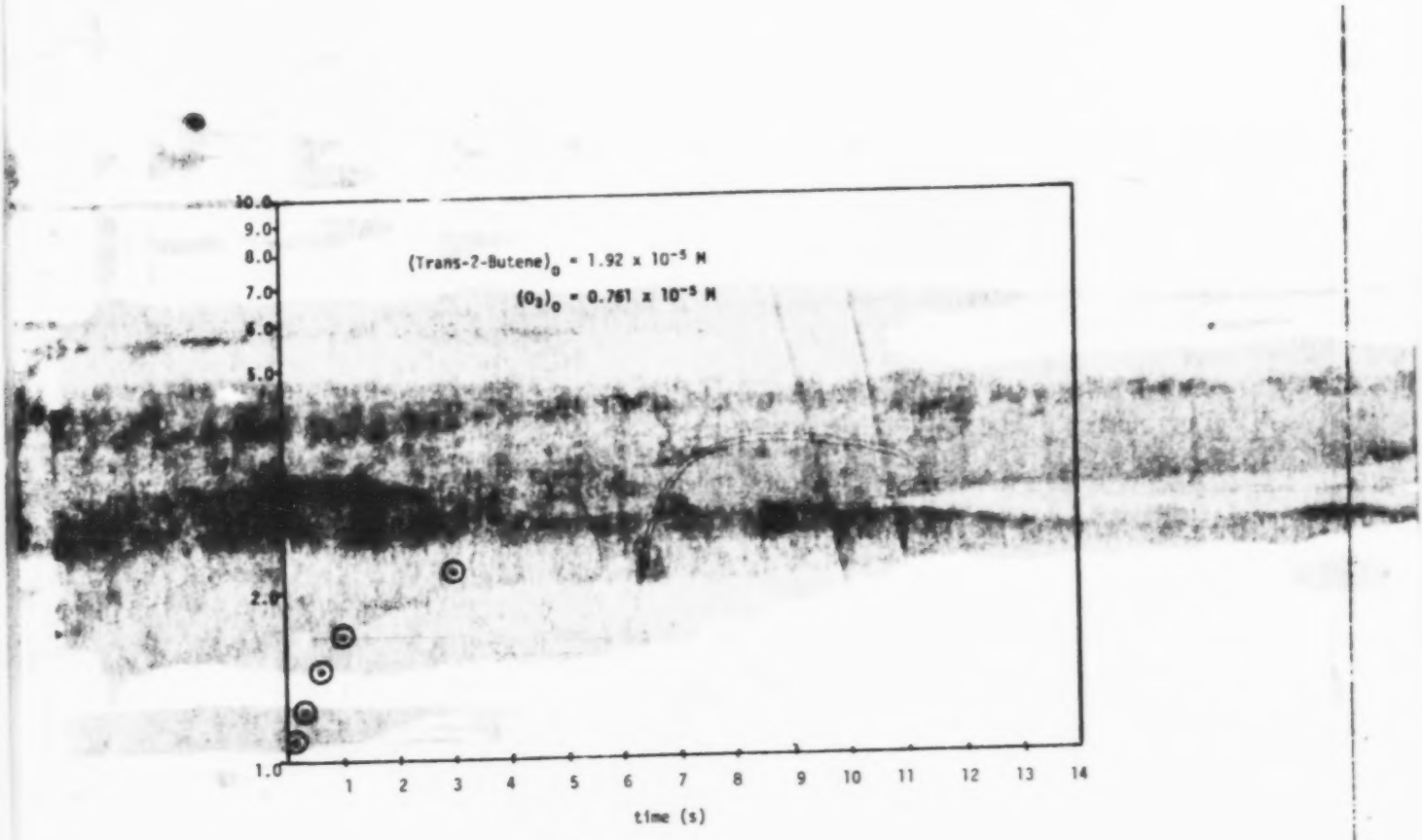

Figure 14. Second Order Plot. Trans-2-butene + Ozone. High Concentration.

Such curvature in the second order rate plots could conceivably be caused by:

1. An inhibition of O_3 decomposition by some complex mechanism
2. Aerosol formation
3. A relatively long-lived intermediate which absorbs the 2537 A radiation nearly as strongly as O_3. The first possibility was tested by an experiment designed as shown in Figure 15.

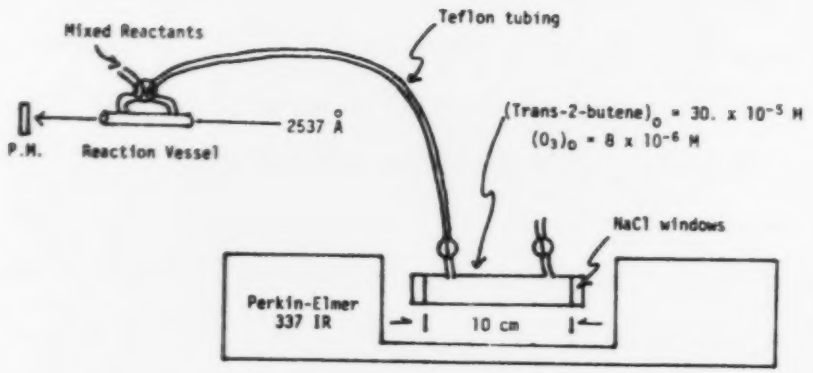

Figure 15. Test for Inhibition of O_3 Decomposition.

The ozone generator was turned on; a steady state condition was reached in the IR cell and the IR spectrum was scanned from 2.5μ to 14μ (1μ = 1 x 10^{-6}m). The O_3 absorption at 9.6μ was no longer detectable, even though the absorbance of the 2537 A line was 0.35 in the reaction vessel. The lowest detectable limit of O_3 was about 10% of the initial O_3. Therefore the absorbance of the 2537 A line in the reaction vessel under these conditions was not due to the presence of O_3. It was therefore concluded that the curvature in the second order rate plot was not due to an inhibition of O_3 decomposition at high trans-2-butene concentrations.

Under these same conditions, the IR spectrum was examined carefully for absorptions not due to those measured for O_3 or trans-2-butene. Infrared absorptions at 3μ, 5.7μ, and 9.1μ were observed to be the strongest signals not due to O_3 or trans-2-butene. When the flow of reactants through the IR cell was stopped, no change in the absorption at any of the three wavelengths above was observed. Therefore, these absorptions in the IR were not due to an unstable intermediate. The observed IR spectrum could be due to a mixture of acetaldehyde, formic acid, water and methanol which are known products from this reaction [8].

To test for light scattering due to aerosol formation, the beam from a He-Ne laser was directed through the reaction vessel during a chemical reaction with $(\text{trans-2-butene})_0$ equal to 30 x 10^{-5} mole/ℓ and $(\text{ozone})_0$ = 8 x 10^{-6} mole/ℓ. A strong Tyndall effect was observed, even though no visible turbidity could be observed in the reaction cell when it was exposed to ordinary room light. The intensity of the Tyndall beam was observed to decrease at about the same rate as the absorbance at 2537 A. Presumably this effect is due to the slow settling of the aerosol particles. It was therefore concluded that the curvature in the rate plots, as shown in Figure 14,

for the case of both trans and cis-2-butene at higher concentrations (c.a. > 5×10^{-6} mole/ℓ) is due to the formation of an aerosol which scatters the 2537 A analysing light. Therefore, reliable rate measurements using this method of analysis are not possible for trans and cis-2-butene above concentrations of about 10^{-5} M since a large fraction of the 2537 A light is scattered by aerosols at these higher concentrations.

After the reaction of trans-2-butene with ozone was run for several minutes at $(\text{trans-2-butene})_o > 1 \times 10^{-5}$ mole/ℓ and $(O_3)_o \approx 10^{-5}$ mole/ℓ, small amounts of liquid were observed to remain in the reaction vessel. The infrared spectrum for this liquid in CCl_4 solvent is shown in Figure 16.

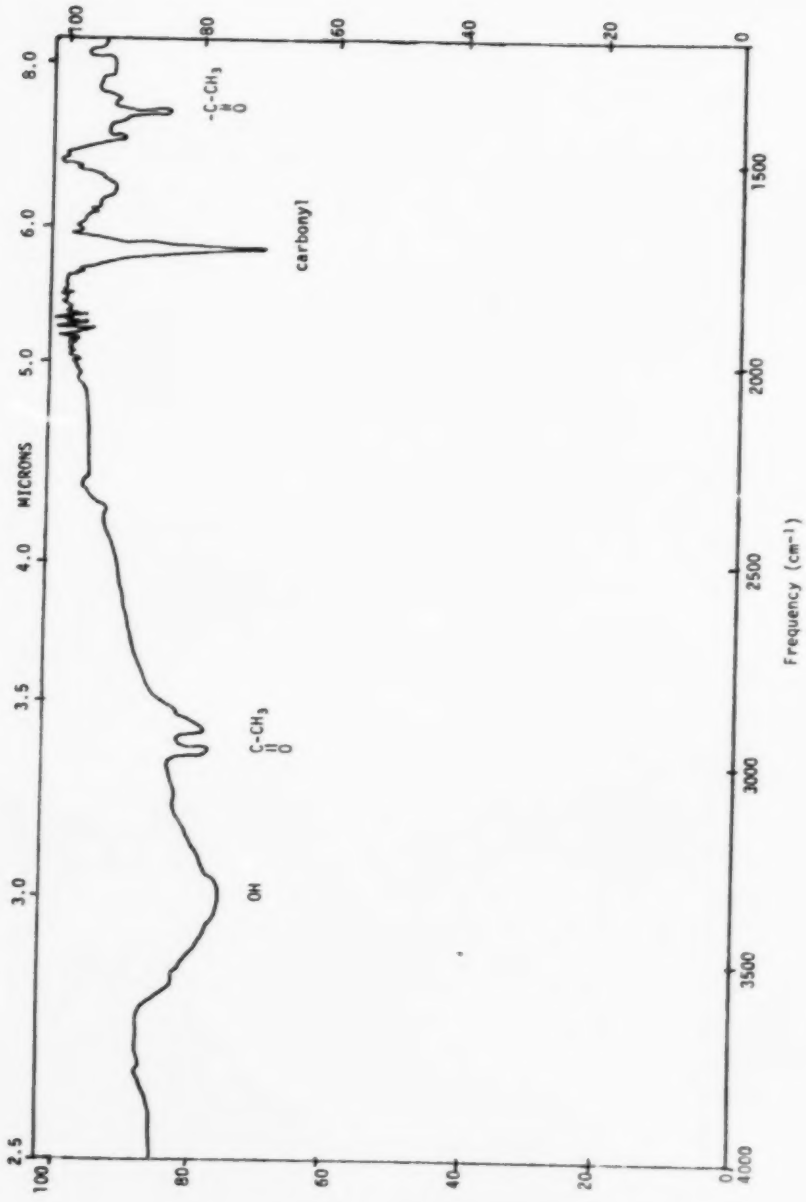

Figure 16a. Infrared Spectrum of the Aerosol From the Trans-2-butene - Ozone Reaction.

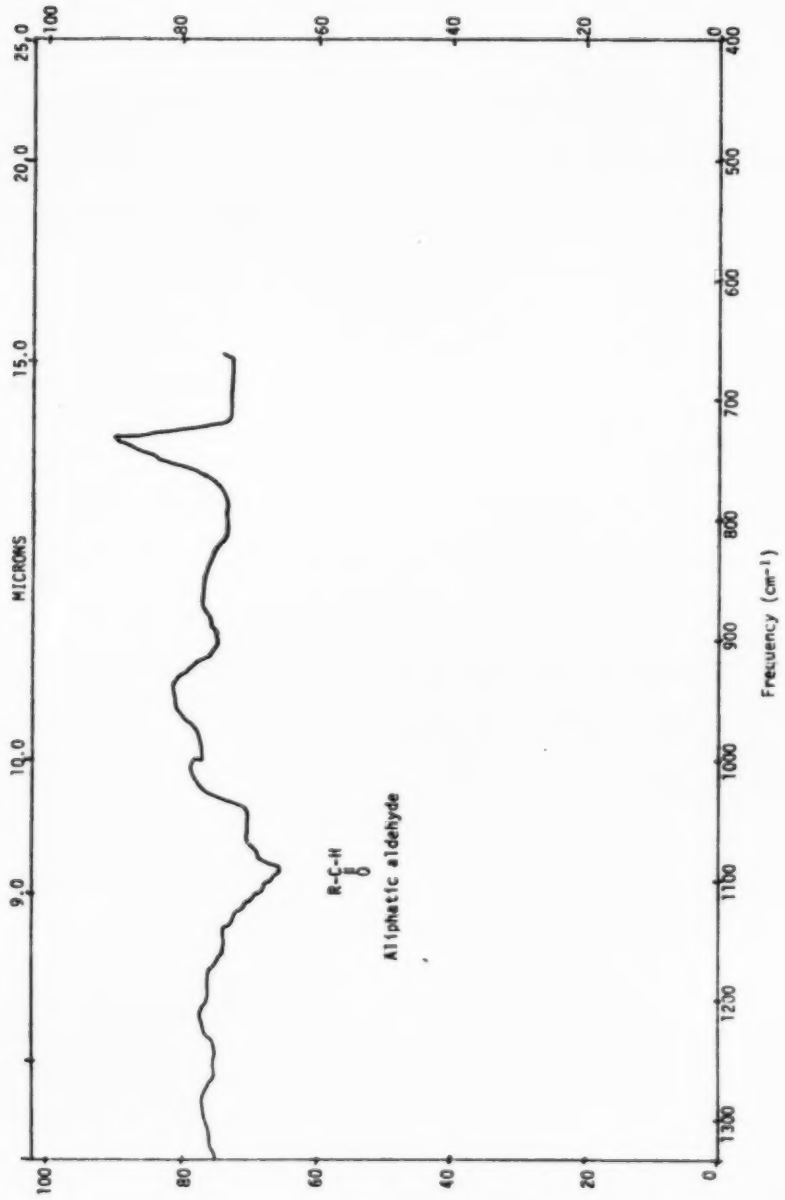

Figure 16b. Infrared Spectrum of the Aerosol From the Trans-2-butene - Ozone Reaction.

The absorptions have been tentatively assigned to the functional groups as listed in Figure 16. This aerosol has not been any further characterized, although such work may be of general interest to further elucidate the reaction mechanism of ozone and trans-2-butene. According to reference 8 products with molecular masses up to 200 Daltons have been found in the aerosol produced in the reaction of ozone and 1-butene. Presumably, the aerosol formed by the reaction of ozone with trans-2-butene contains such high molecular weight components as well.

3. Measurement of light scattering by aerosols in the reaction of trans-2-butene with ozone

Table 6 summarizes the results for a few experiments in which the scattered light was measured as a function of reaction time. The quantity T_I is the induction period which is observed after the flow is stopped and when the first signal from the scattered light is measured. Figure 17 shows the scattered light intensity, Is (in arbitrary units), as a function of reaction time.

TABLE 6

RESULTS OF LIGHT SCATTERING EXPERIMENTS
FOR THE OZONE + TRANS-2-BUTENE REACTION

	$(C_4H_8)_o$	$T_I(s)$	I_{max}	
1.	7.84×10^{-7}M	7.5	19.5	
2.	6.01	11.5 ± 1	9.5 ± 1	
3.	4.88	8. ± 1	7.6	
4.	5.60	8.5 ± 1	13.5 ± 1	
5.	8.04	4.5 ± 1	20. ± 1	
6.	10.9	2.	-	(off scale)
7.	14.1	1.	-	(off scale)
8.	5.18	10.	8.	
9.	8.06	4.5	38.	
10.	8.95	3.	71.	

$(O_3)_o$ = 3.6×10^{-6}M in all runs

T = 298 ± 1°K in all runs

Total Pressure = 760 ± 10 torr in all runs

Total Flow of Gases = ~ 25 ℓ/min

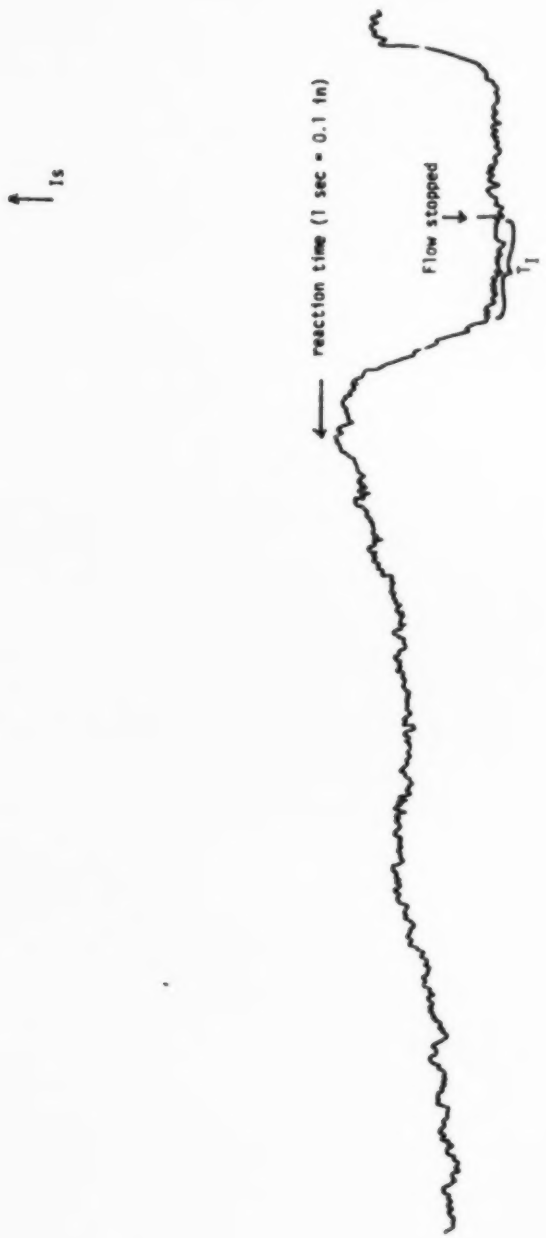

Figure 17. Intensity of Scattered Light vs. Time in the Trans-2-butene + Ozone Reaction.

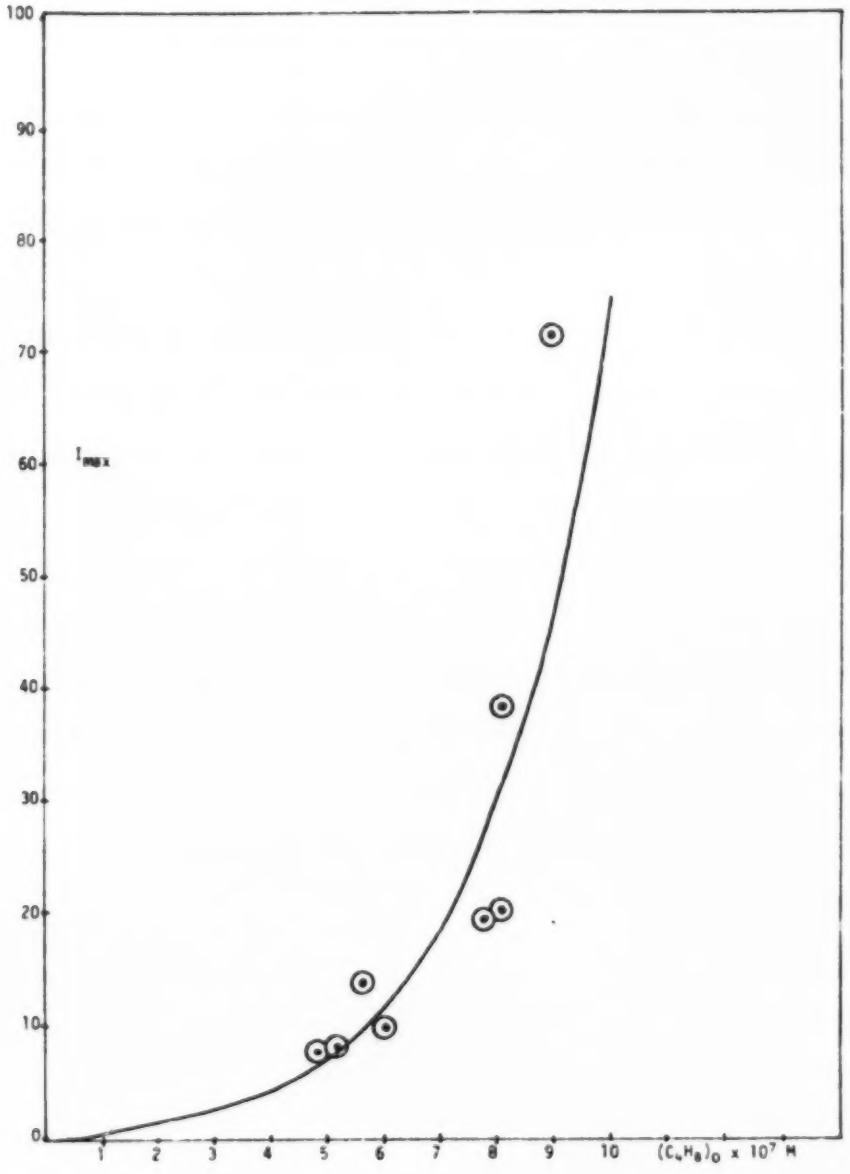

Figure 18. Maximum Intensity of Scattered Light vs. Concentration of Trans-2-butene.

The maximum intensity of the scattered light (I_{max}) is a strong function of initial trans-2-butene concentration as shown in Figure 18. The exponential equation (V)

$$I_{max} = (0.747)\exp\left\{(.4611)\ \frac{(C_4H_8)_o}{10^{-7}}\right\} \qquad (V)$$

where $(C_4H_8)_o$ = trans-2-butene initial concentration describes reasonably well the dependence of I_{max} on $(C_4H_8)_o$ in the range between $(C_4H_8)_o = 5 \times 10^{-7}$ M and $(C_4H_8)_o = 14 \times 10^{-7}$ M. The solid line is equation (V) plotted along with actual data points.

The induction time is also a strong function of the initial concentration of trans-2-butene. Perhaps the induction period exists because sufficient concentrations of products must exist before particles large enough to scatter light strongly enough to be detected are formed.

Exploratory experiments done with ethylene, propene, 1-butene, methylpropene, and cis-2-butene indicate that aerosols are formed in their reactions with ozone. In the case of ethylene, detectable light scattering was observed with $(C_2H_4)_o = 0.44 \times 10^{-5}$ mole/ℓ and $(O_3)_o = 0.75 \times 10^{-5}$ mole/ℓ. Some additional light scattering data are shown for the ethylene-ozone reaction in Table 7. Gas flow rates, total pressure and temperature were the same as described in Table 6.

TABLE 7

LIGHT SCATTERING IN THE ETHYLENE + OZONE REACTION

$(C_2H_4)_o \times 10^5$	$(O_3)_o \times 10^5$	T_I(s)	I_{max}
1.09	0.684	6.	74
0.926	0.629	15.	31
0.439	0.752	20.	16
1.77	0.647	5.	63
1.40	0.703	10.	65
0.840	0.712	7.	38

The rate of settling of aerosol particles formed in the ethylene-ozone reaction was approximated from the rate of decay of intensity of the scattered light. The time required for the scattered light intensity to decrease to one half of the value of the maximum scattered light intensity was taken as the time for the average size aerosol particle to travel the distance equal to the radius of the reaction vessel. Using Stoke's Law (equation VI)

$$V = \frac{2\ r^2\ \rho\ g}{9\ n} \qquad \text{(VI)}$$

where V is the settling rate, r is the diameter of the particle, ρ is the difference in density of the particle and N_2 at 1 atm and 25°C (ρ was approximated as 1 g/cm^3) and n is the viscosity of N_2 under experimental conditions, gives an average particle radius of 1.0μ. This radius is on the same order of magnitude as the radius of particles found in polluted air in the Los Angeles region (9).

SECTION IV

REFERENCES

1. Atkinson, R., B. J. Finlayson, and J. N. Pitts, Jr. Private communication.

2. Bufalini, J. J. and A. P. Altshuller, Can. Jour. of Chem., 43, 2243 (1965).

3. Cox, R. A. and S. A. Penkett, J. Chem. Soc., Faraday Trans. I, 68, 1735 (1972).

4. Hanst, P. L., E. R. Stephens, W. E. Scott and R. C. Doerr, Atmospheric Ozone Olefin Reactions. The Franklin Institute, Philadelphia, Pa. (1958).

5. Johnston, H. S. and H. J. Crosby. J. Chem. Phys., 22, 2243 (1954).

6. Schulten, H. R. and U. Schurath. Private communication.

7. Stedman, D. H., C. H. Wu, and H. Niki, J. Phys. Chem., 77, 2511 (1973).

8. Wei, Y. K. and R. J. Cvetanovic, Can. J. Chem., 41, 913 (1963).

9. Williamson, S..J. Fundamentals of Air Pollution, p. 356. Addison-Wesley Pub. Co. (1973).